Image Processing and wavelets transform for Sizing of Weld Defects Using Ultrasonic TOFD images

Ahmed Kechida, Redouane Drai and Abdelsaalam Benammar

Image and signal processing laboratory. Welding and NDT Centre, Route de Dely-Ibrahim, BP 64, Chéraga, 16035 Alger, Algeria
abs_benammar@yahoo.fr

Ultrasonic Time-Of-Flight Diffraction (TOFD) is rapidly gaining prominence as a reliable non-destructive testing technique for weld inspection in steel structures, providing highly accurate positioning and sizing of flaws. A number of signal and image processing tools have been specifically developed for use with TOFD data and adapted to function autonomously without the need for continuous intervention, configuring automatically according to the nature of the data and the data acquisition settings. This paper presents the results of several innovative procedures based on Multiresolution analysis such as wavelet transforms and texture analysis for detecting edges of planar defects. The approach is based on the decomposition by packets of wavelets of the image while taking into account of the under - image content textural after each level of decomposition. The reconstruction of the image is done by eliminating the under - images of poor textural information and at the end the segmented image is got by Fuzzy c-mean clustering classifier.. The automation positioning of weld flaws in TOFD data as an essential stage of a comprehensive TOFD inspection and interpretation aid is developed and implemented.

Key words: Ultrasonic Time-Of-Flight Diffraction., Texture Analysis, Wavelet Transform, FCMI.

1   Introduction

Non destructive testing possibilities by ultrasonic imagery were hugely improved since new software, able to treat quickly the recorded signals and to create some specific images to this type of test were developed.

At the present time, ultrasonic data acquirements are automatically achieved. Analyses and interpretations are done inductively on cartography called ultrasonic image. The aim is to put to the fore and to characterize flaws in the material. The analysis of ultrasonic images is done manually by an operator. This latest selects images to analyze and research visually the presence of flaws. He then tries to determine precisely the position and the dimensions of these flaws.

Positioning and measuring operation can, at the present time be done by using algorithms and images processing techniques which were the topics of several research projects.

The main objective of the survey is to set up algorithms allowing to the best interpretation data contained in an acquirement.

 Non destructive data processing is at present very widely studied. It allows the exploitation of the information contained in these acquirements. The exploitation of theses information increases the sturdiness of the control tools and often avoids the multiple inspections necessary to detect defects.

This article aims is therefore to study and to develop tools of image processing allowing detecting and localizing edges of planar defects (ex. cracks) present in TOFD images. The achieved algorithm uses information based on the texture defect in an image, partner to wavelet transform. A texture research allows detecting some partially visible flaws by an operator.

2   Time-Of-Flight Diffraction

A relatively recent ultrasonic NDT technique is the Time-of-Flight Diffraction (TOFD) method, which was first described by Silk (1977)[1]. This method relies on the diffraction of ultrasonic energies from 'corners' and 'ends' of internal structures (primarily defects) in a component under test. This is in contrast to conventional pulse echo methods, described above, which rely on directly reflected signals.

The typical apparatus for a TOFD weld examination is shown in Fig.1. Usually a two probe (one transmitter; one receiver) arrangement is used - the chosen transmitter producing a relatively wide beam spread to maximize the extent of the scan. The two probes are aligned geometrically either side of the weld and an A-scan taken at sequential positions along the length of the bead. The time taken to scan a length of weld is therefore very short since no raster scanning at each position is necessary.
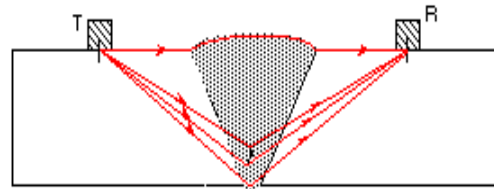
Fig.1 TOFD probes arrangement for weld inspection.

A schematic of an A-scan for the arrangement shown in Fig.2 is given in Fig.3. This shows the detection of four main signals - (1) the surface or lateral signal which travels along the surface of the component and has the shortest arrival time; (2) the top tip of the defect; (3) the bottom tip of the defect; and (4) the backwall echo, which has the longest transit time. Also present in the A-scan are reflections from mode converted signals which have a slower speed of propagation through the specimen and hence a longer transit time. Although mode converted signals are not usually examined in TOFD inspection, they can often duplicate the main body of the A-scan. If both tips of a defect can be resolved in the A-scan then the actual depth and 'through-wall' thickness of the flaw can be accurately calculated (Silk, 1977; Carter 1984). This was the main thrust behind the development of the technique, since other methods, such as standard pulse echo techniques could often locate but not size defects accurately.
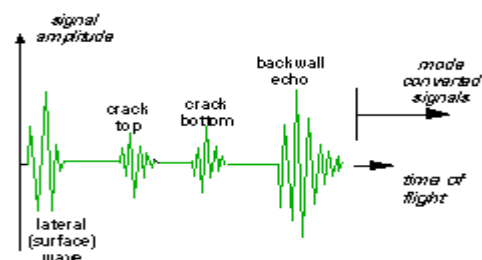
Fig.2 Schematic of TOFD A-scan.
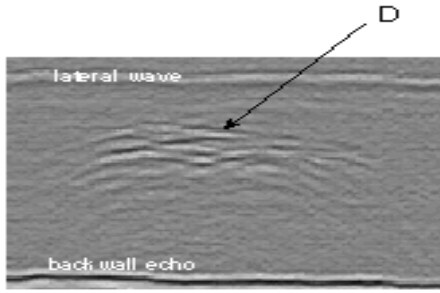
Fig.3 TOFD D-scan of butt weld and defect.

TOFD has some drawbacks in that it is rare to achieve clear signals in the A-scans due to the nature of the weak diffracted signals, coupled with noise, and interference from signals derived from very small pores or non-uniformity in the weld region. However, one of the reasons why TOFD examination has attained widespread use is the associated data acquisition and presentation methodologies proposed very early in its development by Silk (1977). Each A-scan is digitized as it is collected by the receiver, to a resolution of 8 bits - the signal is not rectified and instead is mapped directly to the 256 possible grey levels. A series of A-scans, for a section of weld, is then presented in B or D-scan fashion as shown in the example scan in Fig. 3. In this example scan we can clearly see the lateral wave (at the top), and the mass of backwall echoes (at the bottom). Also present between these signals is a defect, D, around which are peculiar down curved arcs which are typical of TOFD signatures. The arcs are caused by the interaction of the defect with the wide beam spread when the probes are not exactly in line with the flaw - hence the signal becomes progressively stronger near the centre of the arc as the actual position of the defect reaches the centre of the ultrasonic beam. Since the signals associated with the presence of defects are often quite characteristic when shown in Silk's D-scan plot, the TOFD technique is also now extensively employed for defect detection as well as sizing (Silk, 1984), and has also recently been used to completely replace other NDT methods (Verkooijen, 1995).

3   Multirésolution Analysis based on Wavelet Transform

The multirésolution wavelet transform decomposes a signal into the coarser resolution representation which consists of the low frequency approximation information and the high frequency detail information [2]. During the decomposition, the resolution decreases exponentially at the base of 2. Let the convolution of two energy finite functions $f(x,y) \in L^2(R)$ and $g(x,y) \in L^2(R)$ be:

$$(f*g)(x,y) = \int_{-\infty}^{+\infty}\int_{-\infty}^{+\infty} f(u,v)g(x-u,y-v)dudv \qquad (1).$$

The approximation of a two-dimension finite-energy function f(x,y) at resolution 2^j where integer j is a decomposition level, can be characterized by the coefficient calculated by the following convolution :

$$A_{2^j}f = ((f(x,y) \times \phi_{2^j}(-x)\phi_{2^j}(-y))(2^{-j}n,2^{-j}m)_{(n,m)\in Z^2} \quad (2)$$

Where m, n are integers, $\phi(x)$ is a one-dimension scaling function, and $\phi_{2^j}(x) = 2^j\phi(2^jx)$, in general, the $\phi(x)$ is a smooth function whose Fourier transform is concentrated in low frequencies. The difference between approximation information at two consecutive resolutions 2^j and 2^{j-1}, which are characterized by $A_{2^j}f$ and $A_{2^{j-1}}f$, respectively, can be captured by the detail coefficients computed by the following convolutions:

$$D_{2^{j-1}}^1 f = ((f(x,y) \times \phi_{2^{j-1}}(-x)\psi_{2^{j-1}}(-y))(2^{-(j-1)}n,2^{-(j-1)}m)_{(n,m)\in Z^2}$$

$$D_{2^{j-1}}^2 f = ((f(x,y) \times \psi_{2^{j-1}}(-x)\phi_{2^{j-1}}(-y))(2^{-(j-1)}n,2^{-(j-1)}m)_{(n,m)\in Z^2}$$

$$D_{2^{j-1}}^3 f = ((f(x,y) \times \psi_{2^{j-1}}(-x)\psi_{2^{j-1}}(-y))(2^{-(j-1)}n,2^{-(j-1)}m)_{(n,m)\in Z^2}$$

Where $\psi(x)$ is one-dimensional wavelet function and $\psi_{2^j}(x) = 2^j\psi(2^jx)$. The wavelet function $\psi(x)$ is a band-pass filter. $A_{2^j}f$ can be perfectly reconstructed from $A_{2^{j-1}}f, D_{2^{j-1}}^1 f$, $D_{2^{j-1}}^2 f$ and $D_{2^{j-1}}^3 f$.
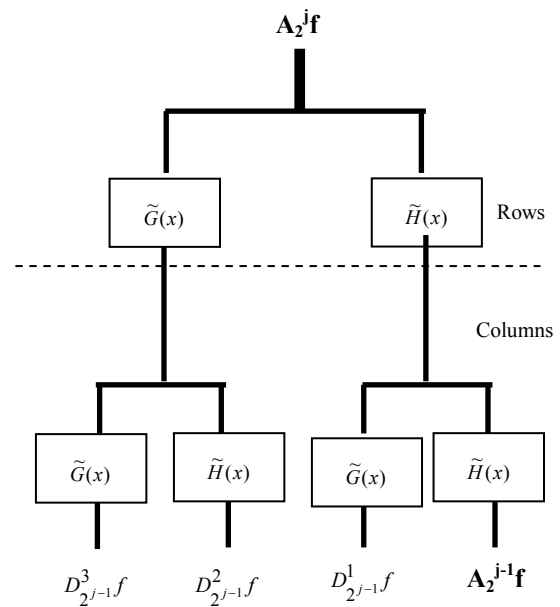
Fig.4 The decomposition of an image

The approximation and detail coefficients can be calculated with a pyramid algorithm based on convolution with two one-dimensional parameter filters. Fig.4 shows the decomposition of $A_{2^j}f$ into $A_{2^{j-1}}f$, $D_{2^{j-1}}^1 f$, $D_{2^{j-1}}^2 f$ and $D_{2^{j-1}}^3 f$. $\tilde{H}$ And $\tilde{G}$ in figure 4 are one-dimension low-pass and one-dimensional high-pass filters, respectively. As figure 4 shows, this algorithm first convolutes the rows of image $A_{2^j}f$ with the one-dimensional filter, retains every other column, convolutes the columns of the resulting signal with another one-dimensional filter and retains every other row. The pyramid decomposition can be continuously applied to the approximation image until the desired coarser resolution 2^{-j} (j>0) is reached.

4   Texture Analysis

Images segmentation method developed in this work, needs a mathematical representation of the textures. These are statistical methods which were selected to carry out this task. One calls statistics attributes the elements characterizing mathematically the textures. They are useful as long as they form the under images classification criteria which only some of them will be kept for further decomposition (they allow the choice of the decomposition channel).

Statistics can be of several orders, but the most used are those of the first and second order. Those of the first order (mean, variance, entropy) cannot characterize the textural aspect of an image so we were interested only to those of the second order.

We than, have a source which is the co occurrence matrix to provide a fourteen indices panel of the possible texture.

The energy and classification criteria are a vector of five of these indices.

The fourteen indices from the co occurrence matrix were calculated by (HARALICK &.., 1973)[3].

After several tests we have opt for the following indices:

- Angular second order moment

$$\sum_{i=1}^{N_g}\sum_{j=1}^{N_g} p(i,j)^2 = \sum_{i=1}^{N_g}\sum_{j=1}^{N_g}\left(\frac{P(i,j)}{R}\right)^2 = \frac{\sum_{i=1}^{N_g}\sum_{j=1}^{N_g} P(i,j)^2}{R^2} \quad (3)$$

- Contrast

$$\sum_{k=0}^{N_g-1} k^2\left(\sum_{i=1}^{N_g}\sum_{j=1}^{N_g}\frac{P(i,j)}{R}\right) = \frac{\sum_{k=0}^{N_g-1} k^2\left(\sum_{i=1}^{N_g}\sum_{j=1}^{N_g} P(i,j)\right)}{R} \quad (4)$$

Avec |i - j| = k.

- Inverse difference moment

$$\sum_{i=1}^{N_g}\sum_{j=1}^{N_g}\left(\frac{p(i,j)}{1+(i-j)^2}\right) \quad (5).$$

- Sum mean

$$\sum_{k=2}^{2N_g}\left(k.p_{x+y}(k)\right) \quad (6).$$

With p_{x+y}(k) = $\sum_{i=1}^{N_g}\sum_{j=1}^{N_g} p(i,j)$ where i + j = k.

- Entropy

$$-\sum_{i=1}^{N_g}\sum_{j=1}^{N_g}\left(p(i,j).\log(p(i,j))\right) \quad (7).$$

Where:

N_g : grey level (in our case N_g=256).

P(i, j) : terms of the not normalised co occurrence matrix .

p(i, j) : terms of the normalised co occurrence matrix .

$$R = \sum_{i=1}^{N_g}\sum_{j=1}^{N_g} P(i,j) \quad (8).$$

5   Segmentation Proposed Algorithm

The segmentation procedure proposed which is based on the multi resolution analysis, consists of the image decomposition using discreet wavelet transform.   For each of the four images we calculate the statistics parameters of the texture (by using the indices defined at the former section), the under image having the more textural information will be selected and decomposed (split up) once again by the discreet wavelet transform using the same procedure until the level 6 of decomposition (splitting up). Then, the reconstruction of the images is done from the three levels 6, 5, and 4 by eliminating the under image holding weak textural information of the last decomposition (split up). At last, we calculate the mean image according to the formula:

$$I_{moy} = \prod_{i=1}^{3} IR_i^2 \quad (9).$$

With IR_i : rebuilt image (i).

The final image is get from a binarisation operation by FCMI Algorithm.

The method of FCMI is a method of supervised classification, it uses the concept of fuzzy logic, and it is given by the following algorithm [6]:

N_c clusters are initialized with random patterns in the features space.

Calculation of the distance between each pattern and each cluster centre:

$$d_{ij} = \left\| x_j - y_i \right\| \quad (10)$$

Calculation of the memberships function μ (**fuzzification**):

$$\mu_{ij} = \left[\sum_{l=1}^{N_c}\frac{d_{ij}^{2/(\beta-1)}}{d_{lj}}\right]^{-1} \quad (11)$$

β is a tuning parameter which controls the degree of fuzziness in the process.

If $d_{lj} = 0$ for $l = l_0$ then $\mu_{l_0 j} = 1$ and ($\mu_{ij} = 0$ for $l \leq i \leq N_c$ and $i \neq l_0$).

The cluster centers change by using the following formula:

$$y_i = \frac{\sum_{j=1}^{m}\mu_{ij}.x_j}{\sum_{j=1}^{m}\mu_{ij}} \quad (12)$$

With m: the number of patterns.

If the new cluster centres are changed, then we move at the stage 2 else we continue.

Defuzzication:

if $\mu_{i_0 j} = \max(\mu_{ij})$ then $\mu_{i_0 j} = 1$ and ($\mu_{ij} = 0$ for $l \le i \le N_c$ and $i \ne l_0$). The form x_j belongs to the class i_0.

In our work we have tow class **'defects' or 'no defects'** and we chose $\beta = 1,03$.

6   Experimentation and results

To check up the strength of the proposed approach we have tested on images realized on an industrial plant.

Fig.5 it is D scan image illustrates the result of the control of a steel block butt weld with three real defects.

Defect D1: opened crack

Defect D2: slag

Defect D3: closed lack of fusion

The result of the first step of the algorithm localizes the lateral back wall wave of the sample and the tree defects. The second step of the algorithm is illustrated by the segmented image obtained (fig.5c), where we can see the development of the defects with regards to the back ground image.

With the same way, we have tested the efficiency of the algorithm on another TOFD image (fig.6). This D scan image illustrates the result of the control of a steel block butt weld with three real defects.

Defect D1: opened crack

Defect D2: slag

Defect D3: closed lack of fusion

Fig.6b and Fig.6c represent respectively the results of two steps of the algorithm: (localization and segmentation). The same remarks should be put to the fore

The results obtained are give satisfactory results. We notice a good detection of the edges of defects.The use of these results for a possible defects dimensioning,. In fact, the image 5c and 6c presents very fine lines characterizing the edges of the defect.

The first problem raised by this kind of images is to localize the echo of the front and those of the back wall of the sample. However we can notice that these areas were detected. Concerning the defects the algorithm is strong enough to allow a proper (correct) detection

5   Conclusion

This paper has addressed the task of automatic positioning and sizing of detected defects in ultrasonic TOFD data as part of a comprehensive automatic interpretation aid.

The proposed approach is based on the decomposition by packets of wavelet. After several tests, we noted that the result was independent from the wavelet choice. For the decomposition canal choice, we have appeal to the statistical textures analysis.

After several tests we have chosen five indexes. Then, the reconstruction is achieved by eliminating coin - images of weak textural information of the last level of decomposition. Finally, the segmented image is obtained by a simple operation of binarisation on the middle image by fuzzy c-means clustering algorithm. witch is calculated from the three pictures rebuilt at different levels.

We consider that the method proposed in this paper is fast and reliable. The combination of these two parameters allows being endowing of a robust and efficient means in detecting flaws from an ultrasonic image of T.O.F.D type in non destructive testing of a material.

References

[1] SHAUN W. LAWSON, GRAHAM A. PARKER, "Automatic detection of defects in industrial ultrasound images using a neural network", *Proc. of Int. Symposium on Lasers, Optics, and Vision for Productivity in Manufacturing I (Vision Systems: Applications)*, June 1996, Proc. of SPIE vol. 2786, pp. 37-47, 1996.

[2] MALLAT S.G., "A theory for multirésolution signal decomposition: the wavelet representation ", *IEEE Trans. on Pattern Analysis and Machine Intelligence,* vol. n°11, July 1989, pp.674-693.

[3] HARALICK R.M., SHANMUGAM K., DINSTEIN I., "Textural features for image classification ", *IEEE Trans. on Systems, Man and Cybernetics, vol. SMC-3, n°6, November 1973, pp.610-621*

[4] SILK, M.G., "The use of diffraction based time-of-flight measurements to locate and size defects", *Brit. J. of NDT*, vol. 26, 1984, pp 208-213.

[5] SILK, M.G., "The use of diffraction based time-of-flight measurements to locate and size defects", *Brit. J. of NDT*, vol. 26, 1984, pp 208-213.

[6] M.FRIEDMAN, A.KANDEL, "introduction to the pattern recognition, statistical, structural, neural and fuzzy logic approaches" Ed imperial college Press 1999.
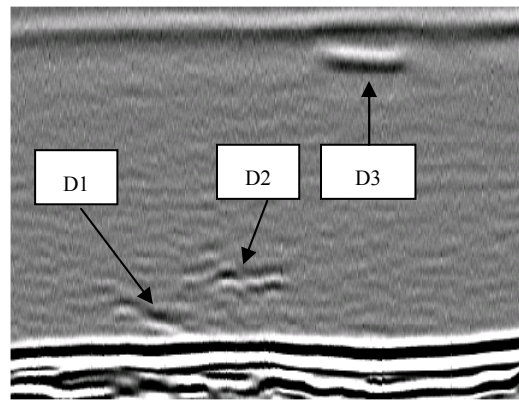
(a)
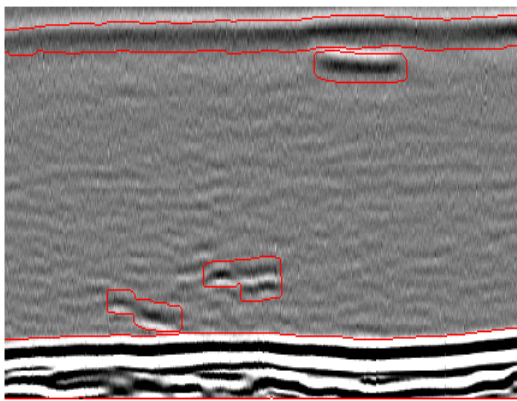
(b)　(c)

Fig.5 Segmentation results of TOFD image (5a).
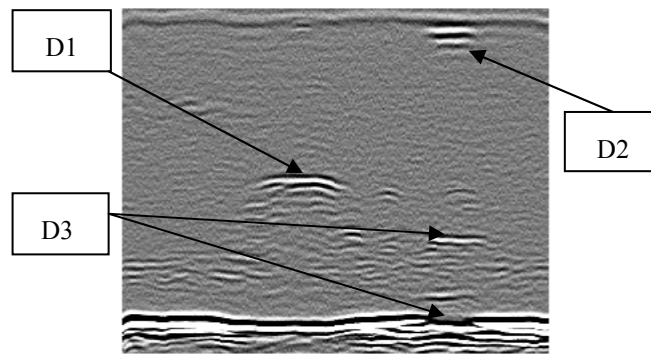
(a)
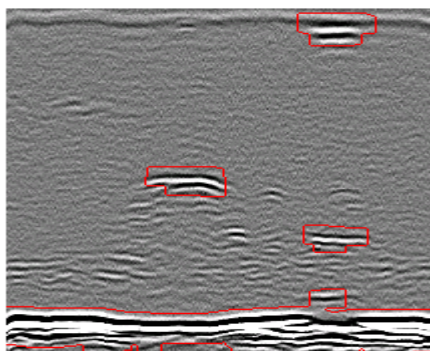
(b)　(c)

Fig.6 Segmentation results of TOFD image (6a).